



ISSN: 0067-2904

Metal Complexes of Adenine Azo Ligand: Synthesis, Identification and Study some of their Applications

Zaid Zuhair Abd^{*}, Alyaa Khider Abbas

University of Baghdad, College of science, Department of chemistry

Received: 13/4/2022 Accepted: 25/3/2023 Published: 30/3/2024

ABSTRACT

This scientific paper presents two novel lanthanide metal complexes [Sm (III) and Ce (IV)] synthesized through a series of reactions involving organic ligand 8-[3-(pyrazoyl)azo]adenine (PAA). Ligand (PAA) and their complexes were characterized using various analytical techniques, including C.H.N.S elemental analysis, magnetic measurement, X-ray diffraction, thermal analysis, SEM, (TGA) UV-Vis spectroscopy, FT-IR spectroscopy, and HNMR analysis. These techniques were employed to support the mode of binding and geometrical structure for ligand (PAA) and its Lanthanide (Ln) complexes. The FTIR and HNMR spectral results showed that (PAA) acts as neutral N,N-bidentate with [Sm (III) and Ce (IV)]. The geometric shape of the synthesized Ln-complexes is octahedral. Also, TGA was used to investigate the thermal behavior of ligand and its complex. The results showed that the ligand dissociated in three steps, while the complex dissociated in five steps. This indicates that the complex is more thermally stable than the ligand, likely due to the formation of strong coordination bonds between the ligand and the metal ions. These findings can contribute to the understanding of the thermal stability of metal complexes and inform the design of new metal-based materials with desirable properties. Finally, this paper examined the antibacterial, antifungal and anticancer activities of PAA and its complexes. The results indicated that all of these compounds exhibited significant activity against bacterial and fungal pathogens, as well as cancer cells.

Keywords: Adenine, azo, antioxidant, antibacterial, cytotoxic effectiveness

المعقدات الفلزية لليكند ادنين-ازو: تحضير وتشخيص ودراسة بعض تطبيقاتها

زيد زهير عبد الامير^{*} ، علياء خضر عباس

جامعة بغداد، كلية العلوم، قسم الكيمياء

الخلاصة

قدم هذه الورقة العلمية معقدين جديدين من معدني اللانثانيدات [Sm (III)] و [Ce (IV)] تم تصنيعهما من خلال سلسلة من التفاعلات التي تتضمن ليكاندات عضوية (PAA) 8-[3-(pyrazoyl)azo]adenine. تم تشخيص الليكند (PAA) و المعقدات المحضرة باستخدام تقنيات تحليلية مختلفة، بما في ذلك تحليل عناصر C.H.N.S، والقياس المغناطيسي، وحيود الأشعة السينية، والتحليل الحراري، (TGA)، SEM، والتحليل الطيفي للأشعة المرئية وفوق البنفسجية، والتحليل الطيفي FT-IR، وتحليل HNMR. تم استخدام هذه التقنيات لدعم طريقة الربط والهيكل الهندسي لليكند (PAA) ومعقدات Lanthanide (Ln) الخاصة به. أظهرت النتائج

*Email: zaid93zuhair@gmail.com

الطيفية FTIR و HNMR أن (PAA) يعمل كاليكند N,N-ثنائي السن مع [Sm (III) و Ce (IV)]. الشكل الهندسي لمجمعات Ln المركبة هو ثماني السطوح. أيضًا ، تم استخدام التحليل الحراري الوزني (TGA) للتحقيق في السلوك الحراري لليكند ومركبته. أظهرت النتائج أن الليكند ينفصل في ثلاث خطوات ، بينما المعقد ينفصل في خمس خطوات. يشير هذا إلى أن المركب أكثر استقرارًا من الناحية الحرارية من الترابط ، ويرجع ذلك على الأرجح إلى تكوين روابط تنسيق قوية بين الترابط والأيون المعدني. يمكن أن تساهم هذه النتائج في فهم الاستقرار الحراري للمعقدات المعدنية وإعلام تصميم مواد معدنية جديدة ذات خصائص مرغوبة. أخيرًا ، فحصت هذه الورقة الأنشطة المضادة للبكتيريا والفطريات والسرطان لـ PAA ومعقداته. أشارت النتائج إلى أن كل هذه المركبات أظهرت نشاطًا جيدًا ضد مسببات الأمراض البكتيرية والفطرية وكذلك الخلايا السرطانية.

1. Introduction

Azo compounds are a class of organic molecules that contain one or more azo (-N=N-) functional groups, which are characterized by a double bond between two nitrogen atoms [1-3]. These compounds have received significant attention due to their diverse structures and unique properties, making them useful in various fields, such as pharmaceuticals [4], biological [5], dyes [6], acid-base indicator [7] and medicines [8]. Azo compounds display remarkable color changes upon reduction or oxidation, making them suitable for colorimetric analysis, and their electron-withdrawing ability allows them to act as good ligands for metal complexes. Furthermore, the introduction of azo groups into a molecule can enhance its solubility, stability, and bioavailability. Lanthanides, also known as rare earth elements, have notable contributions in various fields, including catalysis, optics, and magnetic materials. Their coordination complexes have drawn attention to their potential applications in diverse areas, such as luminescent probes, magnetic resonance imaging contrast agents, and drug design. The distinct properties of lanthanide complexes, such as their large Stokes' shifts, long excited-state lifetimes, and high quantum yields, make them promising fluorophores for bioimaging and sensing purposes. Furthermore, their unique magnetic and electronic properties allow for the design of efficient catalysts, adsorbents, and chemical sensors. Thus, the study of lanthanide coordination chemistry is of significant interest to chemists and researchers who aim to develop functional materials with high applicability in various fields [9,10].

In this study, a novel ligand 8-[3-(pyrazoyl)azo]adenine (PAA) and its Ln-complexes [Sm (III), Ce (IV)] were prepared and identified through various physicochemical, magnetic and spectroscopic techniques as well as thermal analysis was utilized to deduce suggested geometry of the metal ions complexes. Antioxidant and anticancer activity of the ligand (PAA) and [Ce(PAA)₃](SO₄)₂.H₂O complex were studied, also ability to dye wool textiles of ligand and Ln-complex were investigated.

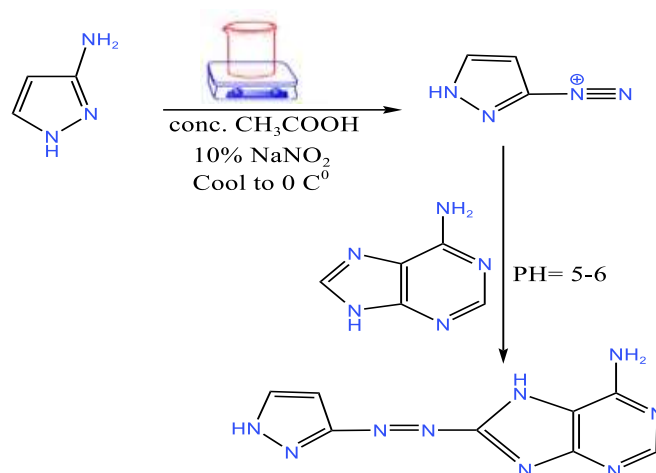
2. Experimental

The chemicals and solvents were purchased including adenine, 3-amino pyrazole, acetone, 10% NaNO₂, 10% NaOH, samarium (III) chloride, and cerium (IV) sulfate from Sigma-Aldrich and were of the highest grade. Micro elemental analysis using the (C.H.N) method was conducted using a (Eure EA 3000 Elemental analyzer). UV-VIS spectra were performed in ethanol using a Shimadzu UV-160A ultraviolet-visible spectrophotometer. FTIR spectra were acquired using CsI discs on a Shimadzu FTIR-8400s Fourier Transform Infrared spectrophotometer (200-4000 cm⁻¹). On a ¹HNMR Spectrometer 400 MHz, Advance III 400 Bruker, Germany, the ¹HNMR spectra were produced using DMSO as the solvent. The pH was measured using the pH Tester and Pocket pH Tester from HANNA devices. Using a HANNA instrument/conductivity tester, complexes (10⁻³ M) in ethanol were examined for conductivity at 25 °C. To determine melting points, a Sturat melting point device was employed. Scanning

electron microscopy (SEM) analysis, electric balance HANNA instruments, radiation ($\lambda=1.54180 \text{ \AA}$), SHIMADZU (XRD) 6000 X-Ray Target Cu K.

2.1 Synthesis of Ligand (PAA)

A ligand called 8-[3-(pyrazoyl) azo] adenine (PAA) has been synthesized using a process that has been published in the literature [11] but with some improvements, as indicated in Scheme 1. 3-aminopyrazole (0.83 g, 0.01mole) was dissolved in 10 mL of distilled water to generate the diazonium salt solution. The cold solution was then mixed with 10 mL of concentrated acetic acid and 10 mL of 10% NaNO_2 , and the mixture was shaken continuously for 30 minutes before cooling to 0°C . An ethanolic alkaline solution of adenine 1.3 gm; 0.01 mole, 10 mL ethanol, 10% NaOH was mixed before the diazonium salt was added. The pH of the solution was adjusted to be between (5-6). Finally, the obtained precipitation was left over night. The resulting brown powder was filtered, and dried using [ethanol: water] [1:1].



scheme 1: synthesis of ligand (PAA)

2.2 Metal complex synthesis

The Ln-complexes were synthesized in a mole ratio of (M: L) (1:3), by adding (0.693 gm; 0.003mole) of the (PAA) ligand in absolute ethyl alcohol to an aqueous solution of metal ion salts [Sm (III) and Ce (IV)] (0.256 gm; 0.001 mole and 0.332 gm; 0.001 mole). After 3 hours of refluxing using ethanol: acetone (3:1) as the solvent, the combined solution's outcome was modified using thin layer chromatography (TLC). The colourful precipitate that produced was filtered, repeatedly washed with water and ethanol (1:1), and then allowed to dry.

2.3 Mole ratio

By applying mole ratio method [12], the ratio of M:L was determined. The interception of two straight lines owing to the mole ratio (M: L).

2.4 Antibacterial and antifungal

The new azo ligand (PAA) and its complexes were examined in vitro for their antibacterial efficacy against two harmful pathogens utilizing a disk diffusion method in ($2 \times 10^{-2}\text{M}$) ethanol as a solvent. Inhibitory zones (measured in mm) were found when the Petri plates were incubated at 37°C for 24 hours (for bacteria) and 72 hours (for fungus) [13] using fluconazole as a fungal control and amoxicillin as a bacterial control. This particular dangerous bacterium was selected depending on its potential to induce a wide range of harmful illnesses in biological systems. The complexes biological activities were examined using two types of bacteria: *Gram-positive* Staphylococcus aureus (Staph), *gram-negative* Klebsiella (E. coli) and one type of

fungi [14].

2.5 Antioxidant

The Following approach which proposed by Sanja et al. [15]. A solution of 0.1 ml of the extract or standard (0.625, 0.125, 0.250, and 0.500 mg/ml) was introduced to a test tube that already contained 3.9 mL of DPPH solution. The absorbance of each solutions was measured at 517 nm using a spectrophotometer after 30 min of incubation at 37 °C. Each measurement was acquired three times.

2.6 Anticancer effectiveness

Tumor cells (1×10^4 - 1×10^6 cells/ml) were cultured on 96 flat well micro-titer plates with a final volume of 200 μ L complete culture medium for each well. Gently shacked parafilm that had been cleaned and wrapped the microplate. Plates were incubated at 37 C° and 5% CO₂ for 24 hours. The medium was taken out, and the necessary concentrations of [Ce(PAA)₃](SO₄)₂.H₂O were serially diluted twice the wells received (6.25, 12.5, 25, 50, 100, and 200 g/mL). Triplicates were used for each concentration and the controls (cells treated with serum free medium). Plates were spent for the chosen exposure duration at 37 Co, 5% CO₂ (24 hours). 10 μ L of the MTT solution were put to each well. At 37 C and 5% CO₂, the plates were then incubated for a further 4 hours. Following incubation, each one was received 100 μ L of the solubilization solution to five minutes before the mediawere carefully removed. By measuring at a 575 nm wavelength using an ELISA reader. To calculate the concentration of chemicals needed to reduce cell viability by 50% for each cell line, optical density data were submitted to statistical analysis[16].

3 Results and discussion

3.1 Physicochemical feature:

The new synthesized yellow-colored azo ligand (PAA) with an adenine core was conceptualized in (scheme 1). All of the synthetic Ln-complexes are soluble in ethanol, methanol, DMF, DMSO. The measurable physical and analytical outcomes were displayed in Table 1. It was discovered that the calculated data and the findings of the elemental analysis were in good agreement, and the metal to ligand ratio (M: L) is (1:3) stoichiometry. Based on the molar conductance measurement, it was assumed that the complexes in (10^{-3} M) ethanol were electrolytic (1:3) in nature.

Table 1: The physicochemical characteristics of the synthesized compounds.

| Comp. (M.wt) (gm/mol) | M:L | Color λ (nm) | % Experimental % (Theoretical) | | | | | | M.P | Δm (S.mol ⁻¹ .cm ²) |
|---|-----|--------------------------|-----------------------------------|------------------|--------------------|----------------|------------------|---------------|------------|--|
| | | | C | H | N | S | M | Cl | | |
| PAA(C ₈ H ₉ N ₉) (231.22) | - | brown322 | 41.51 (41.87) | 3.89 (3.82) | 54.49 (54.88) | - | - | - | 110 C° | - |
| [Sm(PAA) ₃]Cl ₃ .3H ₂ O (1003.02) | 1:3 | Yellow 401 | 28.71 (28.45) | (3.29) (3.89) | (37.68) (37.54) | - | 18.84 19.44 | 10.24 9.75 | 360 C°> | 117.52 |
| [Ce(PAA) ₃](SO ₄) ₂ .H ₂ O (1043.75) | 1:3 | Reddish orange 495 | 27.59 (27.33) | 2.77 (2.22) | 36.21 (36.89) | 6.13 (6.24) | 17.02 (17.24) | - | 360 C°> | 123.44 |

3.2 Natural of the complexes

The most well-known method for identifying the types of complexes formed in solutions that need separation, is the mole ratio approach which was used to investigate the stoichiometric reaction between the ligand (PAA) and [Sm (III) and Ce (IV)] [17]. This method was used to

measure the absorbance versus molar ratio of the (M:L), there is no reliable dissociation while generating the complex, and the plot shows a distinct break when the amount of the ligand (0.25ml) and the amount of the metal ion are changed while remaining constant. This currently displays the make-up of complexes. Figure (1) and (Table 2) were shown that mole ratio (M:L) is (1:3).

Table 2: Mole Ratio of ligand and Ln-complex.

| M:L | Absorbance at λ max (nm) | |
|--------|----------------------------------|-------------------|
| | Sm (PAA) (334) | Ce (PAA) (389) |
| 1:0.25 | 0.251 | 0.244 |
| 1:0.5 | 0.277 | 0.354 |
| 1:0.75 | 0.294 | 0.411 |
| 1:1 | 0.311 | 0.452 |
| 1:1.25 | 0.321 | 0.459 |
| 1:1.5 | 0.325 | 0.462 |
| 1:1.75 | 0.329 | 0.495 |
| 1:2 | 0.355 | 0.522 |
| 1:2.25 | 0.398 | 0.548 |
| 1:2.5 | 0.424 | 0.567 |
| 1:2.75 | 0.456 | 0.582 |
| 1:3 | 0.475 | 0.594 |
| 1:3.25 | 0.493 | 0.610 |
| 1:3.5 | 0.531 | 0.624 |
| 1:3.75 | 0.554 | 0.655 |
| 1:4 | 0.628 | 0.672 |

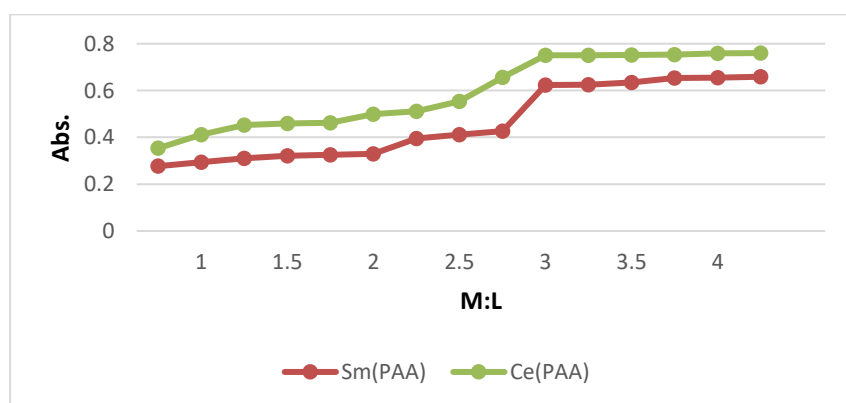


Figure 1: Shows the molar ratio curves for Ln-complexes and PAA-Metal ion solutions at λ_{max} .

3.3 Thermogravimetric analysis (TGA)

The ligand thermal degradation (PAA) and Lanthanides complexes have been discussed by (TGA) in the rang (25-800) C° with argon gas. The suggested formula has been verified using thermal analysis, which was also used to examine the thermal stability of the synthesized ligand

(PAA) with Ln-complexes. The findings appear to be consistent with the formula that the analytical data [18] revealed. According to Figure 2-4 and Table 3, the ligand (PAA) decomposed in three steps, but its complexes did so in five, and there was no mass loss up to 270 °C in the case of the ligand, indicating the presence of moisture. However, in the cases of [Sm (III) and Ce (IV)], the decomposition was up to (22-69 °C) and (25-93 °C), respectively, due to lattice water. The remaining amount of (PAA) is (26.9%), and the thermal stability has resulted in a reduction in the number of Ln- complexes in the following order: [Sm(PAA)₃]Cl₃.3H₂O > [Ce(PAA)₃](SO₄)₂.H₂O

Table 3: The obtained results of TGA for the ligand (PAA) and its Ln-complexes

| Comp. | Molecular Formula (molecular weight) g/mole | Step | TG. Range of The decomposition on (0 C°) | Suggested Assignment | Calculate % | Found % |
|--|--|---------|--|---|-------------|---------|
| PAA | C ₈ H ₉ N ₉ (231.22) | 1 | (22-270) C° | C ₄ H ₉ N _{2.75} | 41.3% | 42.21% |
| | | 2 | (270-360) C° | C ₂ | 10.37% | 10.23% |
| | | 3 | (360-800) C° | C ₂ N _{1.75} | 20.97% | 20.66% |
| | | Residue | <800 C° | N _{4.5} | 27.24% | 26.9% |
| [Sm(PAA) ₃]Cl ₃ .3H ₂ O | SmC ₂₄ H ₃₃ N ₂₇ Cl ₃ O ₃ (1003.02) | 1 | (25-69.73) C° | H ₁₀ O ₃ | 5.78% | 5.95% |
| | | 2 | (69.73-128.91) C° | H ₂₃ Cl ₂ | 9.27% | 10.17% |
| | | 3 | (128.91-214.48) C° | C ₁₃ N ₃ C ₁ | 23.22% | 23.17% |
| | | 4 | (214.48-265) C° | C ₇ N ₃ | 12.56% | 12.80% |
| | | 5 | (265-800) C° | C ₄ N ₉ | 17.34% | 16.97% |
| | | residue | >800 C° | SmN ₁₂ | 31.74% | 30.7% |
| [Ce(PAA) ₃](SO ₄) ₂ .H ₂ O | CeC ₂₄ H ₂₉ N ₂₇ S ₂ O ₉ (1043.75) | 1 | (25-93.16) C° | H ₂₉ C ₃ O | 7.76% | 7.71% |
| | | 2 | (93.16-240) C° | C ₂ N ₇ | 11.68% | 11.84% |
| | | 3 | (240-381.83) C° | C ₆ N | 8.23% | 8.77% |
| | | 4 | (381.83-701.97) C° | C ₁₃ N ₁₀ | 28.35% | 28.54 |
| | | 5 | (701.97-800) C° | N ₆ S ₂ | 14.17% | 14.59% |
| | | residue | <800 C° | CeN ₃ O ₈ | 29.71% | 28.55% |

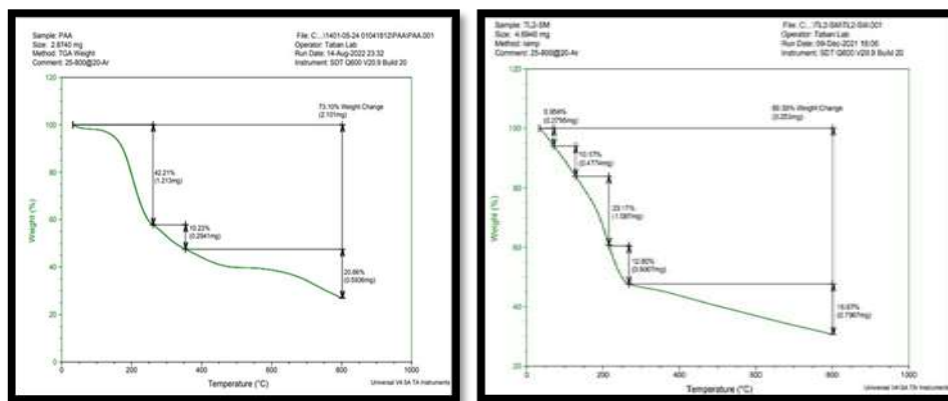


Figure 2: Thermogram for PAA ligand **Figure 3:** Thermogram for the [Sm(PAA)₃]Cl₃·3H₂O complex

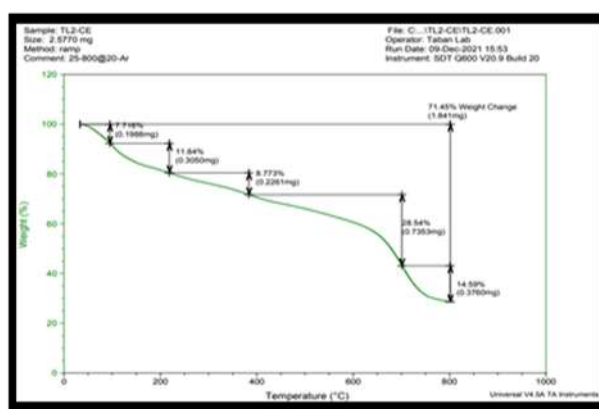


Figure 4: Thermogram for the [Ce(PAA)₃](SO₄)₂·H₂O complex

3.4 The ¹H NMR Spectra of the ligand PAA

Figure 5 shows the ¹H NMR spectra for the free ligand PAA in (DMSO-d₆). A singlet signal at (11.86) ppm is attributed to δ (NH, H) of pyrazole moiety, while at (8.57) ppm is referred to δ (CH) of pyrimidine moiety [19]. The signals at (8.09, 8.25) ppm is represented to (-NH₂, 2H) in adenine [20], while the chemical shift at (8.45) ppm was returned to δ (-NH) in imidazole moiety [21]. The multi signals were featured at (7.00-7.9) ppm was belonged to proton of naphthalene ring [22].

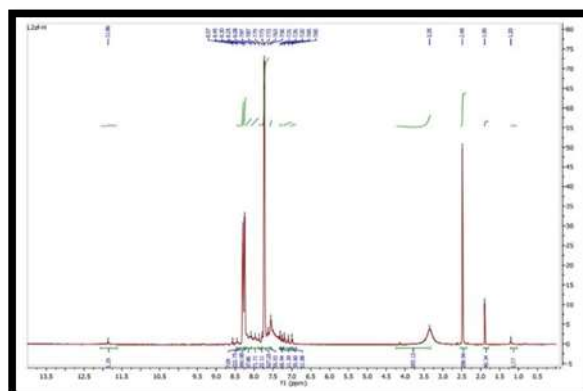


Figure 5: ¹H NMR Spectrum for the PAA ligand

3.5 Electronic spectra and magnetic properties

The UV-Vis spectra of the free ligand (PAA) in ethanol solvent [10^{-4}] reveals two bands at (274 nm, 36496.35 cm^{-1} and 322 nm, 31152.65 cm^{-1}), which were ascribed to ($\pi \rightarrow \pi^*$) The azo moiety was used as a transition for intramolecular charge transfer (Figure 6) [23]. The electronic spectra (UV-Vis) of the [Sm (III) and Ce (IV)] complexes were displayed in Figures 7 and 8, and the data was included in Table 4. Both a chromic shift and an absorption band are brought on by chelating to lanthanide ions. The bulk of lanthanide ions absorb electromagnetic radiation because of the partially filled 4f- orbital, especially in the visible region of the spectrum, which excites the ions from their ground state to the higher electronic state. Electric radiation and magnetic dipoles can both excite f-f transitions. Unlike the magnetic dipole transitions, which are frequently parity-allowed and invisible, the electric dipole transitions are parity prohibited (Laporte-forbidden) and considerably weaker. Due to their great weakness and destruction by the severe band absorption (PAA), these transitions were consequently omitted from the spectra of Ln-complexes [24]. The two compounds have paramagnetic magnetic characteristics.

Table 4: Electronic spectra for the ligand (PAA) and it's Ln – complexes

| Compound | $\lambda_{\text{max}}(\text{nm})$ | Absorption band (cm^{-1}) | Transition | Geometry |
|----------------------|-----------------------------------|--------------------------------------|---------------------------|----------|
| PAA | 274 | 36496.35 | $(\pi \rightarrow \pi^*)$ | - |
| | 321 | 31152.65 | $(\pi \rightarrow \pi^*)$ | - |
| [Sm(PAA)3]Cl3.3H2O | 401 | 24937.66 | C.T | O.h |
| [Ce(PAA)3](SO4)2.H2O | 495 | C.T | O.h | |

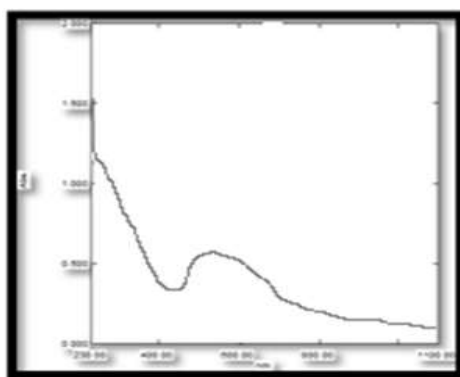


Figure 6: Ligad PAA

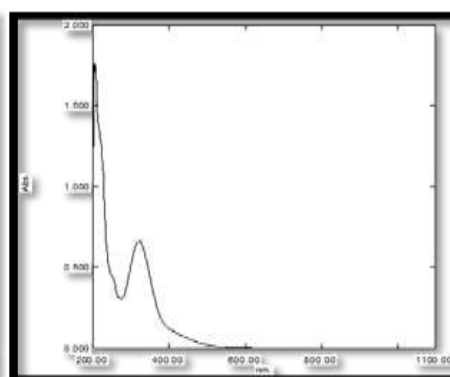


Figure 7: PAA+Ce

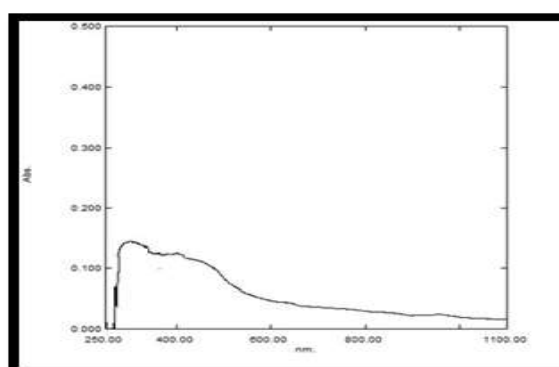


Figure 8: PAA+Sm

3.6 FT-IR spectra of PAA ligand and its complexes

To ascertain how the ligand and its complexes are coordinated, use the principal FT-IR vibration bands shown in Table 5 for the (PAA) ligand and its complexes. Figures 9-11 show the range of wavelengths within which their spectra were obtained.

the spectra of the Sm (III) and Ce (IV) complexes, the most significant band for the azo compound is the azo moiety in the free ligand, which appeared at $(1413) \text{ cm}^{-1}$ and was displaced to higher wavelength at $(1423 \text{ and } 1423) \text{ cm}^{-1}$, demonstrating that the pair of electrons on the nitrogen atom for the azo moiety is a state of coordination with the metal ion [25]. As a result, when compared the spectrum of a free ligand (PAA), the strength of this band in the complexes was decreased [26]. The FT-IR spectrum of the free ligand (PAA) was assigned doublet band for the asymmetric and symmetric (NH_2) moiety this band was unchanged in the spectra of complex (**Table 5**). showing that there was no chelating via this moiety, but that a slight alteration in position or form was occasionally ascribed to a fall in or rise in resonance as a result of chelating [26], while the imine moiety ($\text{C}=\text{N}$) for the imidazole ring in adenine was referenced by the ligand (PAA) $(1701-1687) \text{ cm}^{-1}$. Due to coordination with the metal ion, this band was shifted to its maximal wavelength in the region of $(1733 \text{ and } 1745) \text{ cm}^{-1}$ in the spectra of Sm(III) and Ce(IV) complexes [27]. The bands were attributed to $\nu(\text{C}=\text{N})_{\text{pyr.}}$ and $\nu(\text{C}=\text{N})_{\text{prm.}}$ have little effected on complexation [28] [**Table 5** and (**Figure 9-11**)]. The spectra of Sm (III) and Ce (IV) complexes were recorded new bands in the $(432-437) \text{ cm}^{-1}$ and $(669-653) \text{ cm}^{-1}$ respectively, which were belong to $\nu(\text{Ln}-\text{N}_{\text{azo}})$ and $(\text{Ln}-\text{N}_{\text{imd.}})$ [26]. According to the information provided above, the ligand (PAA) acts as a neutral N,N-bidentate through the azo and imidazole moiety of adenine.

Table 5: vibration bands of the (PAA) ligand and its complexes

| Assessment center | $\nu(\text{N}-\text{H})$ | $\nu(\text{C}=\text{N})_{\text{pyr.}}$ | $\nu(\text{C}=\text{N})_{\text{imd}}$ | $\nu(\text{C}=\text{N})_{\text{pyrm.}}$ | $\nu(\text{N}=\text{N})_{\text{azo}}$ | $\nu(\text{M}-\text{N})_{\text{azo}}$ | $\nu(\text{M}-\text{N})_{\text{imd.}}$ |
|----------------------|--------------------------|--|---------------------------------------|---|---------------------------------------|---------------------------------------|--|
| PAA | 3355 st. 3431 b,st | 1639 sh,m | 1701 d,m 1687 d,m | 1558 st. | 1413 st,sh | - | - |
| [Sm(PAA)3]Cl3.3H2O | 3367 b,st 3400 b, st. | 1633 sh,m - | 1733 | 1546 st. | 1423 m. . | 437 w. | 669 w. |
| [Ce(PAA)3](SO4)2.H2O | 3487 b,m 3452 b,m | 1620 sh,m - | 1745 | 1546 m. | 1423 w. | 432 | 653 sh,m |

s=strong, m=medium, w=weak, sh=sharp, prm.=Pyrimidine , imd.=Imidazole , pyr=Pyrazole

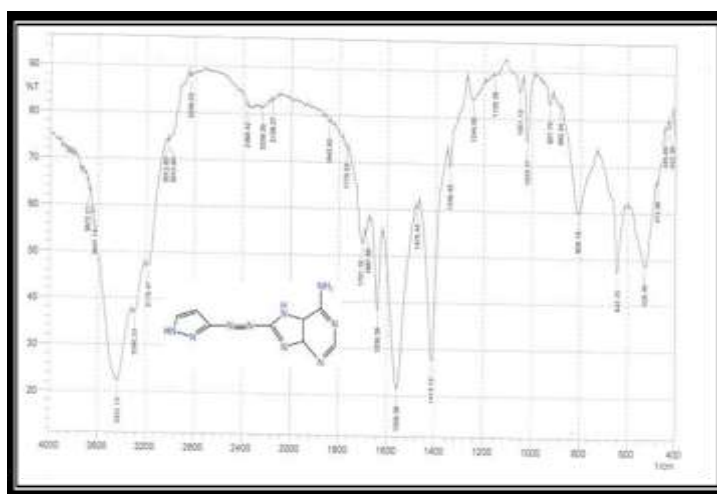


Figure 9: FTIR spectrum of (PAA) ligand

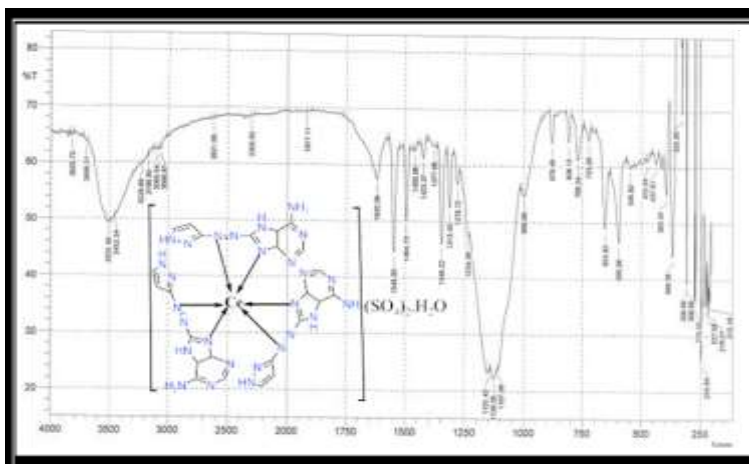


Figure 10: FTIR spectrum of $[\text{Ce}(\text{PAA})_3](\text{SO}_4)_2 \cdot \text{H}_2\text{O}$

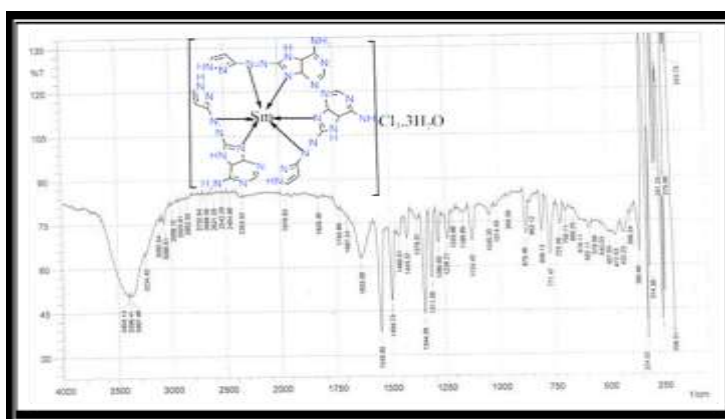


Figure 11: FTIR spectrum of $[\text{Sm}(\text{PAA})_3]\text{Cl}_3 \cdot 3\text{H}_2\text{O}$.

3.7 Assess of powder X-ray diffraction

Figures 12-14 show the three strongest reflection peaks for the (PAA) ligand, $[\text{Sm}(\text{PAA})_3]\text{Cl}_3 \cdot 3\text{H}_2\text{O}$ and $[\text{Ce}(\text{PAA})_3](\text{SO}_4)_2 \cdot \text{H}_2\text{O}$ in the range of 2θ (11.1415-12.2355), (31.8205-45.6042), and (31.4135-14.6576), respectively. In accordance with this information, the semi-crystalline nature and particle size of (PAA) ligand and their Ln-complexes were estimated from XRD patterns based on the highest intensity value compared with the other bands using the Renewed Debye-Teller method [28-29]. The main characteristic reflection peak for (PAA) ligand occurs at (11.1415) in the diffraction pattern of (PAA) ligand, while these band occurs at (31.8205) and (31.4135) of $[\text{Sm}(\text{PAA})_3]\text{Cl}_3 \cdot 3\text{H}_2\text{O}$ and $[\text{Ce}(\text{PAA})_3](\text{SO}_4)_2 \cdot \text{H}_2\text{O}$ respectively.

$D = K \lambda / \beta \cos \Theta$ Where:

D: the main size of crystalline domains, which may be equal or smaller to the crystal grain size (the apparent particle size of the grains) and war represented as volume function by (A) or (nm) unite.

β = full width at half maximum (FWHM) of X-ray diffraction peak .

θ = Bragg angle $\lambda = 0.15406 \text{ nm}$

K = 0.9 (Constant)

Table 6 represents the Data from X-ray diffraction, including the Bragg angle value (2θ), full width at half maximum (FWHM), and particle size (D). The number of particles per (PAA), [Sm(PAA)₃]Cl₃.3H₂O and [Ce(PAA)₃](SO₄)₂.H₂O are (0.1322 nm , 0.6214 nm and 0.441 nm) respectively. These values were emphasized that particle size is located within the nanoscale range. The interplanar spacing (d) was calculated from the status of intense peak according to Bragg's equation [30].

$n\lambda = 2d \sin \theta$ where:

$\lambda = 0.15406 \text{ \AA}$

n= integration number

d= is the spacing of the crystal layers (path difference)

θ = is the incident angle (the angle between incident ray and the scatter plane)

The (d) data calculated and observed for (SAA), [Sm(PAA)₃]Cl₃.3H₂O and [Ce(PAA)₃](SO₄)₂.H₂O are (7.9412, 2.8102 and 2.8455) \AA respectively.

Table 6: Particle size of ligands (PAA) and their complexes

| Compounds | 2θ (deg) | FWHM (nm) | d (\AA) (Calculated) | d (\AA) (Found) |
|--|--------------------|--------------|------------------------------------|-------------------------------|
| PAA | 11.1415 | 0.86 | 7.9412 | 7.9351 |
| [Sm(PAA) ₃]Cl ₃ .3H ₂ O | 31.8205 | 0.2224 | 2.8102 | 2.8099 |
| [Ce(PAA) ₃](SO ₄) ₂ .H ₂ O | 31.4135 | 0.3239 | 2.8455 | 2.8454 |

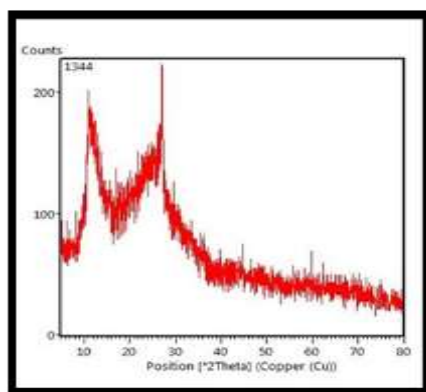


Figure 12: (PAA) ligand

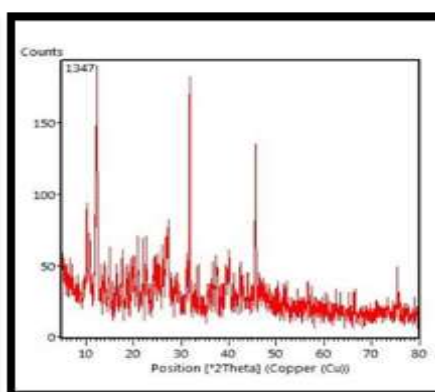


Figure 13: [Sm(PAA)₃]Cl₃.3H₂O

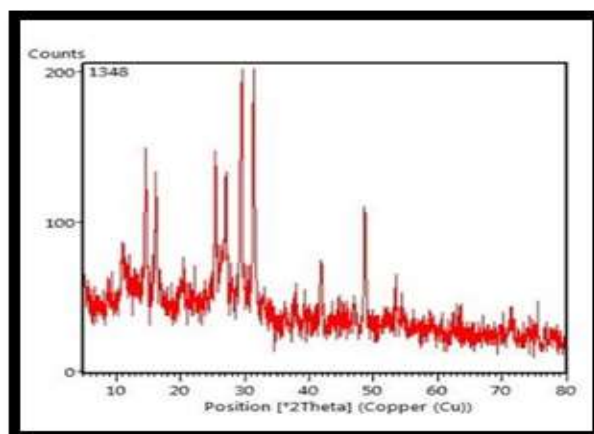


Figure 14: [Ce(PAA)₃](SO₄)₂.H₂O

3.8 SEM analysis

The $[\text{Sm}(\text{PAA})_3]\text{Cl}_3 \cdot 3\text{H}_2\text{O}$ complex and its ligand (PAA) surface morphology were investigated. Some information will get about the surface topography and composition of sample [31]. The SEM images for the ligand (PAA) and (Sm) complex, respectively, are shown in Figures 15–16. The ligand (SAA) was observed in the SEM image to be aggregated, spherical, nonuniform, and to have a smooth surface with an average ($D=33.19\text{nm}$) [32]. As $[\text{Sm}(\text{PAA})_3]\text{Cl}_3 \cdot 3\text{H}_2\text{O}$, it has been depicted as aggregated, spherical, and non-uniform particles with a smooth surface and an average ($D=72.67\text{ nm}$) in the SEM image.

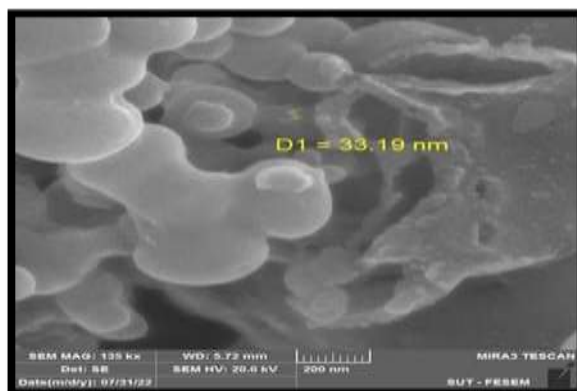


Figure 15: SEM analysis for the PAA ligand

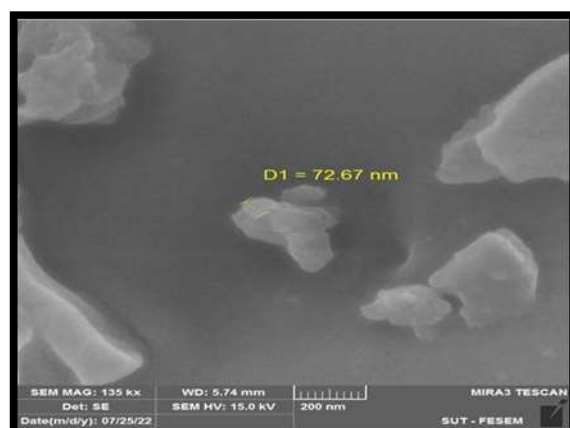


Figure 16: SEM analysis for the $[\text{Sm}(\text{PAA})_3]\text{Cl}_3 \cdot 3\text{H}_2\text{O}$

3.9 Scavenging activity on DPPH radicals

Antioxidants were assumed to be efficient in scavenging DPPH radicals because of their ability to donate hydrogen [34]. The stable free radical DPPH may absorb an electron from a hydrogen radical to create a diamagnetic molecule. The antioxidant-induced drop in DPPH radical absorbance at 517 nm was utilized to calculate the reduction in DPPH radical. The ability of a material to behave as a hydrogen donor or free-radical scavenger, as well as the antioxidant activity of foods and plants, have all been evaluated using the DPPH reaction. [34]. By employing DPPH radical scavenging activity, (PAA) ligand and its metal complex $[\text{Ce}(\text{PAA})_3](\text{SO}_4)_2 \cdot \text{H}_2\text{O}$ shown in vitro antioxidant activity. A positive control ascorbic acid was used. At concentrations of 12.5 mg/mL of (PAA) and $[\text{Ce}(\text{PAA})_3](\text{SO}_4)_2 \cdot \text{H}_2\text{O}$, (37.35 ± 1.226) and (40.43 ± 3.877) respectively. $[\text{Ce}(\text{PAA})_3](\text{SO}_4)_2 \cdot \text{H}_2\text{O}$ complex. At the concentration 200 mg/mL, DPPH radical scavenging activity increased dramatically to (76.70 ± 0.483) and (84.84 ± 2.994) for (PAA) ligand and $[\text{Ce}(\text{PAA})_3](\text{SO}_4)_2 \cdot \text{H}_2\text{O}$ respectively. **Tables**

7 and 8 list the results of DPPH radical scavenging activity of (PAA), [Ce(PAA)₃](SO₄)₂.H₂O and vitamin C **Figures 17 and 18** show the results.

Table 7: DPPH radical scavenging activity of (PAA) ligand and vitamin C

| Concentration(mg/ml) | DPPH Radical Scavenging Activity (Mean ± SD; %) | |
|----------------------|---|-------------|
| | PAA | Vitamin C |
| 12.5 | 37.35±1.226 | 22.23±0.409 |
| 25 | 44.28±3.108 | 37.00±2.646 |
| 50 | 52.00±1.365 | 55.60±2.285 |
| 100 | 72.11±0.644 | 72.73±0.933 |
| 200 | 76.70±0.483 | 84.03±1.753 |

Table 8 : DPPH radical scavenging activity of [Ce(PAA)₃](SO₄)₂.H₂O and vitamin C

| Concentration (mg/ml) | DPPH Radical Scavenging Activity (Mean ± SD; %) | |
|-----------------------|--|-------------|
| | [Ce(PAA) ₃](SO ₄) ₂ .H ₂ O | Vitamin C |
| 12.5 | 40.43±2.238 | 42.20±1.408 |
| 25 | 52.31±1.518 | 57.91±3.423 |
| 50 | 67.17±0.2278 | 65.20±2.567 |
| 100 | 79.82±3.075 | 78.67±1.850 |
| 200 | 84.84±2.994 | 85.03±0.598 |

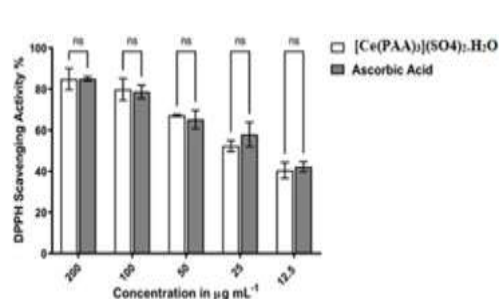
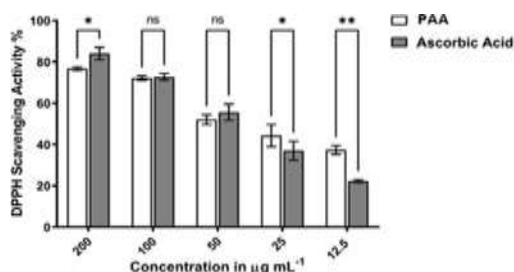


Figure 17: scavenging activity of (PAA) ligand **Figure 18:** scavenging activity of [Ce(PAA)₃](SO₄)₂.H₂O

3.1 30/3/2024 Cytotoxic effectiveness

The cytotoxic impact of [Ce(PAA)₃](SO₄)₂.H₂O on the leukemia cancer cell line (THP-1) was assessed [35]. The cell vitality and inhibition rate of the tumour cell line were determined by the MTT

test

using different dosages of the chemical [Ce(PAA)₃](SO₄)₂.H₂O). The fraction of live cells was evaluated in comparison to the untreated cell line HdFn [36]. Cytotoxic effects of water At doses between 12.50 and 400 g/mL, the THP-1 cell line demonstrated a dose-dependent decrease in cell viability as shown in Table 9. Cell viability is decreased as [Ce(PAA)₃](SO₄)₂.H₂O concentration is raised. The greatest THP-1 cell viability was found at 12.50g/mL (95.181.28), while the lowest THP-1 cell viability (percentage) was found at 400 g/mL (48.234.57). [Ce(PAA)₃](SO₄)₂.H₂O was found to have the most powerful cytotoxic impact, with an IC₅₀ of (51.68) g/ mL. The effect of

[Ce(PAA)₃](SO₄)₂.H₂O on the HdFn normal cell line produced an IC₅₀ of (124.9) g/ mL. Figure 19. We deduce from the IC₅₀ values that the [Ce(PAA)₃](SO₄)₂.H₂O complex requires a low concentration to kill the THP-1 cell line, while still having an impact on normal cells (HdFn). The influence of [Ce(PAA)₃](SO₄)₂.H₂O complex in killing cancer cells depends on its morphological properties motivated cell death and DNA damages, this causes a metal ion chelated with DNA at the (N7) of the guanine and adenine bases, preventing transcription and blocking DNA [37]

Table 9: Cytotoxicity effect of [Ce(PAA)₃](SO₄)₂.H₂O on THF-1 and HdFn cells after 24 hours incubation at 37 °C.

| [Ce(PAA) ₃](SO ₄) ₂ .H ₂ O (µg/mL) | THP-1 cell line viable cell count Mean± S.D. | HdFn cell line's viable cell count Mean± S.D. |
|--|--|---|
| 400.00 | 48.23 ± 4.57 | 71.18 ± 0.69 |
| 200.00 | 54.98 ± 2.03 | 78.24 ± 1.53 |
| 100.00 | 63.77 ± 3.71 | 84.34 ± 2.66 |
| 50.00 | 75.27 ± 4.26 | 95.33 ± 1.18 |
| 25.00 | 86.19 ± 3.92 | 95.22 ± 0.82 |
| 12.50 | 95.18 ± 1.28 | 95.18 ± 0.41 |

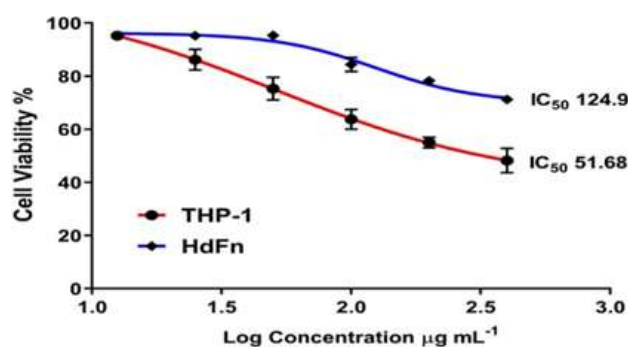


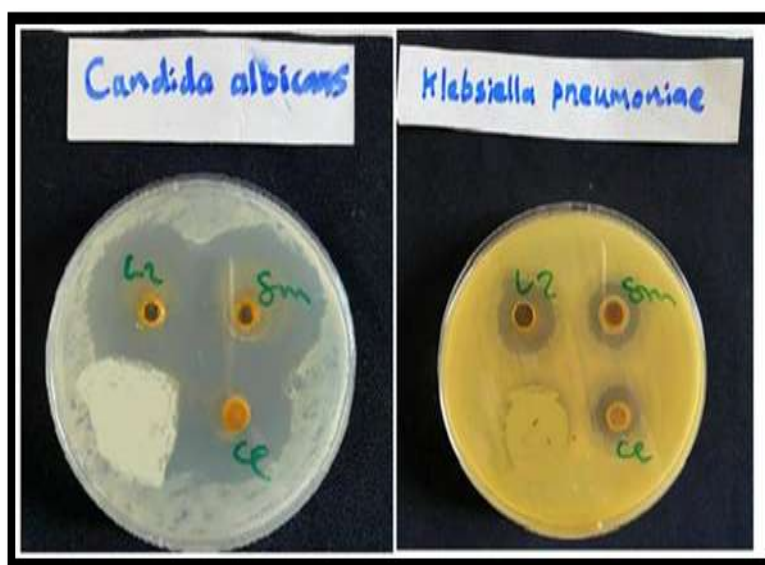
Figure 19: Cytotoxic effect of [Ce(PAA)₃](SO₄)₂.H₂O on THP-1 and HdFn cells after a 24-hour incubation period at 37 degrees Celsius

3.10 Antibacterial and antifungal Activity

Metal ions may interact with a particular ligand in live tissues, inhibiting chelating sites and interfering with normal functions [38]. The growth and metabolism of biological systems are significantly impacted by metal ions, as well. Metal complexes may be used in medicine to deliver ligands, metal ions, or both to a known location in the biological system [39]. A variety of researchers are interested in azo compounds because of their many pharmacological and molecular properties [40]. The findings are shown in Table 10. The Ln-complexes were discovered to have moderate action against Amoxicillin, a reference antibiotic that efficiently suppressed the same harmful microorganisms. Expect the free ligand to exhibit potent anti-Amoxicillin action as well as potent anti-Candida activity for the free ligand (PAA) and their complexes, as shown in Figure 20

Table 10: The inhibitory zones for ethanol, Amoxicillin, fluconazole, ligand (PAA), and their complexes are measured in millimeters.

| Compounds | Staphylococcus aureus (Staph) Gram-positive | Klebsiella (E. coli) gram-negative | Candida |
|----------------------|--|---------------------------------------|---------|
| Ethanol | - | - | - |
| Amoxicillin | 14 | 15 | - |
| fluconazole | - | - | 20 |
| PAA | 22 | 22 | 33 |
| [Sm(PAA)3]Cl3.3H2O | 10 | 16 | 34 |
| [Ce(PAA)3](SO4)2.H2O | 11 | 15 | 30 |

**Figure 20:** activity of ligand and Ln-complexes with Candida and Klebsiella

Conclusion

After spectral and analytical physicochemical studies on the ligand (PAA) and its complexes, several conclusions have been drawn and establish the following points: The ligand (PAA), which acted as a neutral N, N-bidentate chelating ligand that bonded to the target lanthanide metal ions, was produced by mildly altering the diazotization procedure. An octahedral chelating complex is formed by the nitrogen atoms of imidazole in the adenine and the nitrogen atom of azo [Sm(III), Ce(IV)]. It was discovered through X-ray diffraction research that the ligand and its complexes both had nanoscale characteristics. Both the ligand and the complexes have various antibacterial and antifungal activities. The Ce (IV) compound and (PAA) ligand have antioxidant and anticancer activities.

References

- [1] Kılınçarslan, R., Erdem, E., Kocaokutgen, H, "Synthesis and spectral characterization of some new azo dyes and their metal complexes", *Transition Met. Chem*, Vol. 7, pp. 102-106, 2017.
- [2] Abbas, N., Tirmizi, S.A., Shabir, G., Saeed, A., Hussain, G., Channer, P.A., Saleem, R., Ayaz, M, "Chromium(III) complexes of azo dye ligands: Synthesis, characterization, DNA binding and application studies", *Inorg. Nano-Met. Chem*, Vol. 48, pp. 57-66, 2018.
- [3] O.I. Lipskikh, E.I. Korotkova, Ye.P. Khristunova, J. Barek, B. Kratochvil, "Sensors for voltammetric determination of food azo dyes - a critical review", *Electrochimica Acta*, Vol. 260, pp. 974-985, 2018.
- [4] Sroor M. Kadhim, Saad M. Mahdi, "Preparation and Characterization of New (Halogenated Azo-Schiff) Ligands with Some of their Transition Metal Ions Complexes". *Iraqi Journal of Science*, Vol. 63, pp. 3283-3299, 2022.
- [5] Zainab Amer Sallal, Hasan Thamer Ghanem, "Synthesis and Identification of New Oxazepine Derivatives bearing Azo group in their structures". *Iraqi Journal of Science*, Vol. 59, pp. 1-8, 2018.
- [6] H. Etesami, M. Mansouri, A. Habibi, F. Jahantigh, "Synthesis and investigation of double alternating azo group in novel para-azo dyes containing nitro anchoring group for solar cell application", *J. Mol. Struct.*, Vol. 1205, pp. 127432, 2019.
- [7] Noor Adel Hussein, Alyaa Khider Abbas, "Synthesis, spectroscopic characterization and thermal study of some transition metal complexes derived from caffeine azo ligand with some of their applications", *Eurasian Chem. Commun*, Vol. 4, pp. 66-92, 2021.
- [8] Suaad M.H. Al-Majidi, Mohammed G.A Al-Khuzai. "Synthesis and Characterization of New Azo Compounds Linked to 1,8-Naphthalimide and Studying Their Ability as Acid-Base Indicators", *Iraqi Journal of Science*, Vol. 60, pp. 2341-2352, 2019.
- [9] Chr. Klixbüll Jørgensen, "Electron transfer spectra of lanthanide complexes", *Molecular Physics*, Vol. 5, pp. 271-277, 1962.
- [10] D.J. Jasim, Alyaa.K. "Synthesis, identification, antibacterial, medical and dyeing performance studies for azosulfamethoxazole metal complexes", *Eurasian chemical communication*, Vol. 4, pp. 16-40, 2022.
- [11] Alyaa Khider Abbas. "SYNTHESIS, SPECTROSCOPIC, THERMAL AND BIOLOGICAL STUDIES OF SOME NOVEL METAL IONS COMPLEXES", *International Journal of Applied Sciences and Technology*, Vol. 4, pp. 322-338, 2022.
- [12] Schweiger MJ, Beck W., "Metal Complexes of Biologically Important Ligands, Part CLXXVIII. Addition of the Pentacarbonylrhenium Cation [(OC)5Re]+ to the Xanthine Alkaloids Caffeine, Theophylline, and Theobromine", *Zeitschrift für anorganische und allgemeine Chemie*, Vol. 21, pp. 1335-1337, 2017.
- [13] Jain R, Singh R, Kaushik NK., "Synthesis, characterization, and thermal and antimicrobial activities of some novel organotin (IV): Purine base complexes", *Journal of Chemistry*, Vol. 2013, pp. 1-12, 2013.
- [14] Sanja, S.D., Sheth, N.R., Patel, N.K., Dhaval, P. and Biraju, P. "Characterization and evaluation of antioxidant activity of portulaca oleracea", *Int. J. Pharm. Pharm. Sci*, Vol 1, pp. 74-84, 2009.
- [15] Yifeng He, Qiuqing Zhu, Mo Chen, Qihong Huang, Wenjing Wang, Qing Li, Yuting Huang, Wen Di, "The changing 50% inhibitory concentration (IC50) of cisplatin: a pilot study on the artifacts of the MTT assay and the precise measurement of density-dependent chemoresistance in ovarian cancer", *Oncotarget*, Vol. 7, pp. 70803-70821, 2016.
- [16] Abbas, Alya Khider, Rafal Salam Kadhim, "Metal Complexes of Proline-Azo Dyes, Synthesis, Characterization, Dyeing Performance and Antibacterial Activity Studies" *Orient J Chem*, Vol. 33, pp. 402-417, 2017.
- [17] Issa, Y. M., W. F. El-Hawary, A. F. A. Youssef, and A. R. Senosy, "Spectrophotometric determination of sildenafil citrate in pure form and in pharmaceutical formulation using some chromotropic acid azo dyes", *Spectrochimica Acta Part A-molecular and Biomolecular Spectroscopy*, vol. 75, pp. 1297-1303, 2010.
- [18] Karcı F, Demirçalı A, Şener İ, Tilki T. "Synthesis of 4-amino-1H-benzo [4, 5] imidazo [1, 2-a] pyrimidin-2-one and its disperse azo dyes. Part 1: Phenylazo derivatives", *Dyes and Pigments*, Vol.

- 71, pp.90-96, 2006.
- [19] Huo Y, Lu J, Hu S, Zhang L, Zhao F, Huang H, Huang B, Zhang L. "Photoluminescence properties of new Zn (II) complexes with 8- hydroxyquinoline ligands: dependence on volume and electronic effect of substituents", *Journal of Molecular Structure*, Vol. 1083, pp. 144-151, 2015.
- [20] Husham M. Hasan Mubark, Israa N.Witwit, Abid Allah M. Ali, " Synthesis of new azo imidazole ligand and fabricating it's chelate complexes with some metallic ions", *Journal of Physics: Conference Series*, Vol. 1660, pp.1-9, 2020.
- [21] Yasuyuki Matsushita · In-Cheol Jang · Takanori Imai Kazuhiko Fukushima · Seung-Cheol Lee, " Naphthalene derivatives from Diospyros kaki", *The Japan Wood Research Society*, Vol. 56, pp. 418-421, 2010.
- [22] Dinçalp H, Toker F, Durucasu İ, Avcıbaşı N, İcli S. "New thiophene-based azo ligands containing azomethinegroup in the main chain for the determination of copper (II) ions". *Dyes and Pigments*, Vol. 75, pp. 11-24, 2007.
- [23] Alya Khider Abbas, "Lanthanide Ions Complexes of 2-(4-amino antipyrine)-L-Tryptophane (AAT): Preparation, Identification and Antimicrobial Assay". *Iraqi Journal of Science*, Vol 56, pp. 3297-3309, 2015.
- [24] Mallikarjuna NM, Keshavayya J, Maliyappa MR, Ali RS, Venkatesh T. "Synthesis, characterization, thermal and biological evaluation of Cu (II), Co (II) and Ni (II) complexes of azo dye ligand containing sulfamethaxazole moiety", *Journal of Molecular Structure*, Vol. 1165, pp. 28-36, 2018.
- [25] Alyaa Khider Abbas, Wafaa Waleed AL-Qaysi. " Synthesis and Characterization of Novel Nano Azo Compounds as a New pH Sensor", *Arabian Journal for Science and Engineering*, Vol. 48, pp. 399-415, 2023.
- [26] Essam M.S. , Nagwa M.M. H. " Synthesis and Antimicrobial Evaluation of Some Pyrazole Derivatives", *Molecules*, Vol. 17, pp. 4962-4971, 2012.
- [27] Silverstein RM, Webster FX, Kiemle DJ. "Spectrometric Identification of Organic Compounds, 7th editio" John Wiley & Sons, 2005.
- [28] S. Junaid S. Qazi; Adrian R. Rennie; Jeremy K. Cockcroft; Martin Vickers, "Use of wide-angle X-ray diffraction to measure shape and size of dispersed colloidal particles", *J.colloid interface sci*, Vol. 338, pp. 2009.
- [29] N. F. Abbas and A. K. Abbas, " Novel complexes of Thiobarbituric acid-azo dye: structural, spectroscopic, biological activity and dyeing, *Biochem. Cell. Arch*, Vol. 20, pp. 2419-2433, 2020.
- [30] E.N.masten, A.G.Fox and M.A.Keefe., "international tables for crystallography", *Kluwer Academic*, Dordect, 2004.
- [31] Jedidi I, Khemakhem S, Saïdi S, Larbot A, Elloumi-Ammar N, Fourati A and Amar, "Preparation of a new ceramic microfiltration membrane from mineral coal fly ash: Application to the treatment of the textile dying effluents", *Powder Tech*, Vol. 208, pp. 427-432, 2011.
- [32] Rambabu, D., C.P. Pradeep and A. Dhir, "Al³⁺-Phenanthroline Xerogel for Dual Application: Catalyst for Knoevenagel Condensation and Fluorescent Chemosensor for Azo Dyes". *Chemistry Select*, vol, pp. 3371-3376, 2016.
- [33] T.C.P. Dinis, V.M.C. Madeira, L.M. Almeida, Arch. "Action of Phenolic Derivatives (Acetaminophen, Salicylate, and 5-Aminosalicylate) as Inhibitors of Membrane Lipid Peroxidation and as Peroxyl Radical Scavengers", *Archives of Biochemistry and Biophysics*, vol. 315 pp. 161-169, 1994.
- [34] Gerlier, D. and N. Thomasset, "Use of MTT colorimetric assay to measure cell activation", *Journal of immunological methods*, vol. 94, pp. 57-63, 1986. 1986.
- [35] A. Taş, S. Şahin-Bölükbaşı, E. Çevik, E. Özmen, E. Gümüş, Y. Siliğ. " An in vitro Study of Cytotoxic Activity of Euphorbia macroclada boiss on MCF-7 Cells", *Indian J. Pharm. Educ. Res*, vol. 52, pp. 119-123, 2018.
- [36] Kasparkova J, Kostrhunova H, Novakova O, Křikavová R, Vančo J, Trávníček Z, Brabec V. "A photoactivatable platinum (IV) complex targeting genomic DNA and histone deacetylases". *Angewandte Chemie International Edition*, vol. 54, pp. 14478-14482, 2015.
- [37] El-Ghamry HA, Fathalla SK, Gaber M. "Synthesis, structural characterization and molecular modelling of bidentate azo dye metal complexes: DNA interaction to antimicrobial and anticancer activities". *Applied Organometallic Chemistry*, vol. 3, pp. 1-13, 2018
- [38] Ahluwalia VK, Kaur J, Ahuja BS, Sodhi GS. "Organomercury (II) complexes of 6-thioguanine:

- synthesis, characterization, and biological studies", *Journal of inorganic biochemistry*, Vol. 42, pp. 147-151, 1991.
- [39] Özerkan D, Ertik O, Kaya B, Kuruca SE, Yanardag R, Ülküseven B. "Novel palladium (II) complexes with tetradentatethiosemicarbazones. Synthesis, characterization, in vitro cytotoxicity and xanthine oxidase inhibition", *Investigational new drugs*, vol.37, pp. 1187-1197, 2019.
- [40] Jain R, Singh R, Kaushik NK. "Synthesis, characterization, and thermal and antimicrobial activities of some novel organotin (IV): Purine base complexes", *Journal of Chemistry*, vol. 2, pp. 1-12, 20.